THESIS

GRAVITY CONSTRAINTS ON EXTENSION AND MAGMATISM IN THE NORTHERNMOST RIO GRANDE RIFT, NORTHERN COLORADO

Submitted by

Jorge Andrés Espinoza Celi

Department of Geosciences

In partial fulfillment of the requirements

For the Degree of Master of Science

Colorado State University

Fort Collins, Colorado

Summer, 2025

Master's Committee:

Advisor: Dennis Harry

Derek Schutt
Yoichiro Kanno

ABSTRACT

GRAVITY CONSTRAINTS ON EXTENSION AND MAGMATISM IN THE NORTHERNMOST RIO GRANDE RIFT, NORTHERN COLORADO

The Rio Grande Rift (RGR) is a north-trending belt of extensional basins extending from southern New Mexico to central Colorado, where its physiographic expression ends. Opening of the RGR initiated in the late Oligocene forming a series of rift basins linked by accommodation zones where the amount of extension increases southward. This thesis tests the hypothesis that RGR related extensional processes can be found further north in Colorado where basins such as Middle Park, North Park and Sand Wash are located. In this region, extensional features are more broadly distributed up to the southern edge of the Wyoming craton near the Wyoming state border. To evaluate the hypothesis, gravity data from the PACES dataset was complemented by 192 new gravity measurements. This data was used to calculate a Free Air Anomaly map and construct a forward gravity model to constrain lithosphere and upper asthenosphere density structure.

The results are illustrated along three E-W oriented cross sections cutting Middle Park, the Rabbit Ears Range and North Park. The observed gravity field along these profiles correlate with the topography, showing higher gravity values over the Park Basins and the Front and Park Ranges. Lower gravity values are observed west of the Park Basins in the Sand Wash Basin and Uinta Basin areas. The calculated gravity field from the density model reveal, large amplitude, long wavelength gravity misfits showing a gravity overestimation in the Park Basins region and underestimation near the Colorado-Utah state border. These misfits were reduced by adding igneous features at various depths within the lithosphere and lateral density and thickness variations in the crust. Beneath the Park Basins region, the igneous features in the forward model are smaller and more felsic toward the north which supports lithospheric thinning and decompression

melting with more advanced extension towards the south consistent with the southward increase in RGR extension observed in its main rift basins. The results correlate with seismic evidence from previous studies showing shallowing in the lithosphere-asthenosphere boundary and low Vp and Vs in northern Colorado. The results point to the northern Colorado region being part of the RGR system but at a less mature stage of rifting compared to the main RGR rift basins found further south.

ACKNOWLEDGEMENTS

I would like to express my sincere gratitude to my advisor, Dr. Dennis Harry, for his mentorship, patience and insights provided throughout all stages of my research work. Thank you for strengthening my enthusiasm for geophysics research and helping shape my academic path. Also, I would also like to thank the members of my thesis committee, Dr. Derek Schutt and Dr. Yoichiro Kanno, for their time and guidance in the development of this thesis.

I am also thankful to the Department of Geosciences at Colorado State University and all the professors who taught me during my Master's degree. Special thanks to my lab colleague Micah Mayle for his critical input and advice throughout my work.

Finally, I am profoundly grateful with the Fulbright program, sponsored by the United States Department of State, for believing in me and supporting my educational journey. This has been the opportunity of a lifetime and has allowed me to grow as both a geologist and a person.

TABLE OF CONTENTS

1. INTRODUCTION

The Rio Grande Rift (RGR) is a classic example of a continental rift. Its physiographic expression extends from Leadville in central Colorado to Chihuahua in Mexico and separates the Colorado Plateau in the west from the Great Plains in the east (Keller & Baldridge, 1999) (***Figure 1***). The opening of the RGR was synchronous along its length and initiated in the late Oligocene (Abbey & Niemi, 2018). Throughout its more than 1,000 km of length, the RGR is formed by a series of half grabens that alternate from west-tilted to east-tilted which are linked by accommodation zones (Abbey & Niemi, 2020; Keller & Baldridge, 1999). The RGR can be subdivided into the North RGR (San Luis, upper Arkansas River and Blue River Basins), Middle RGR (Alburquerque and Española Basins) and South RGR (The Palomas, Jornada and Tularosa Basins) with reduced extension in the northern basins in comparison to the southern basins (***Figure 2***).

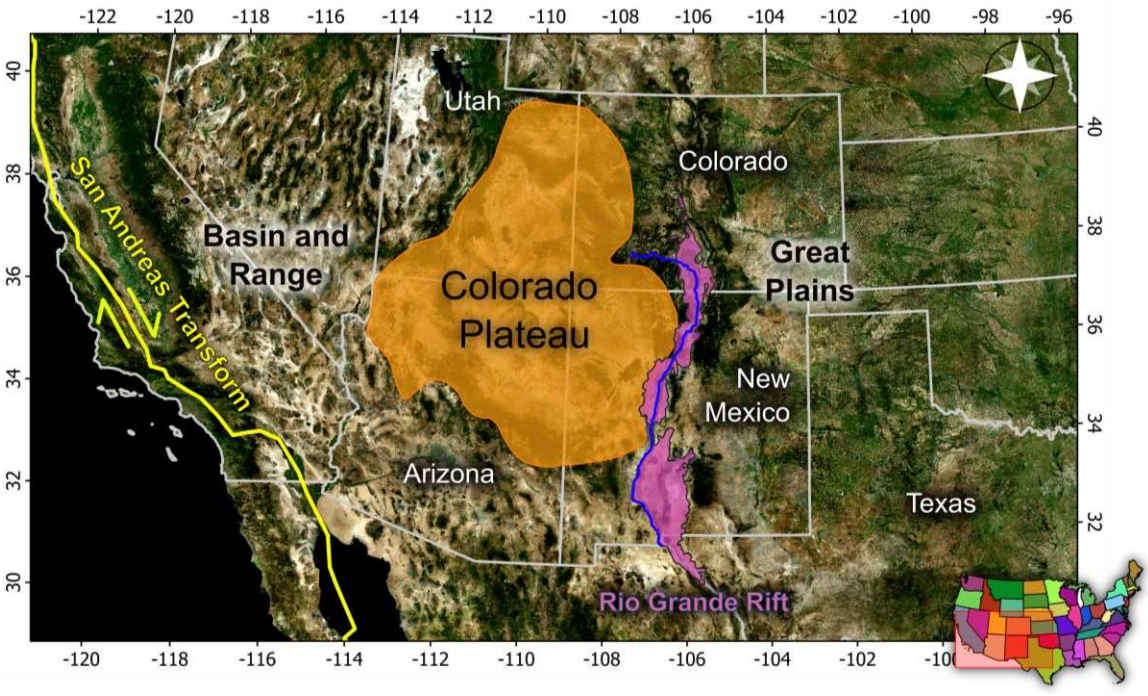

Figure 1: Location and extent of the Rio Grande Rift (RGR) in North America and related physiographic features.

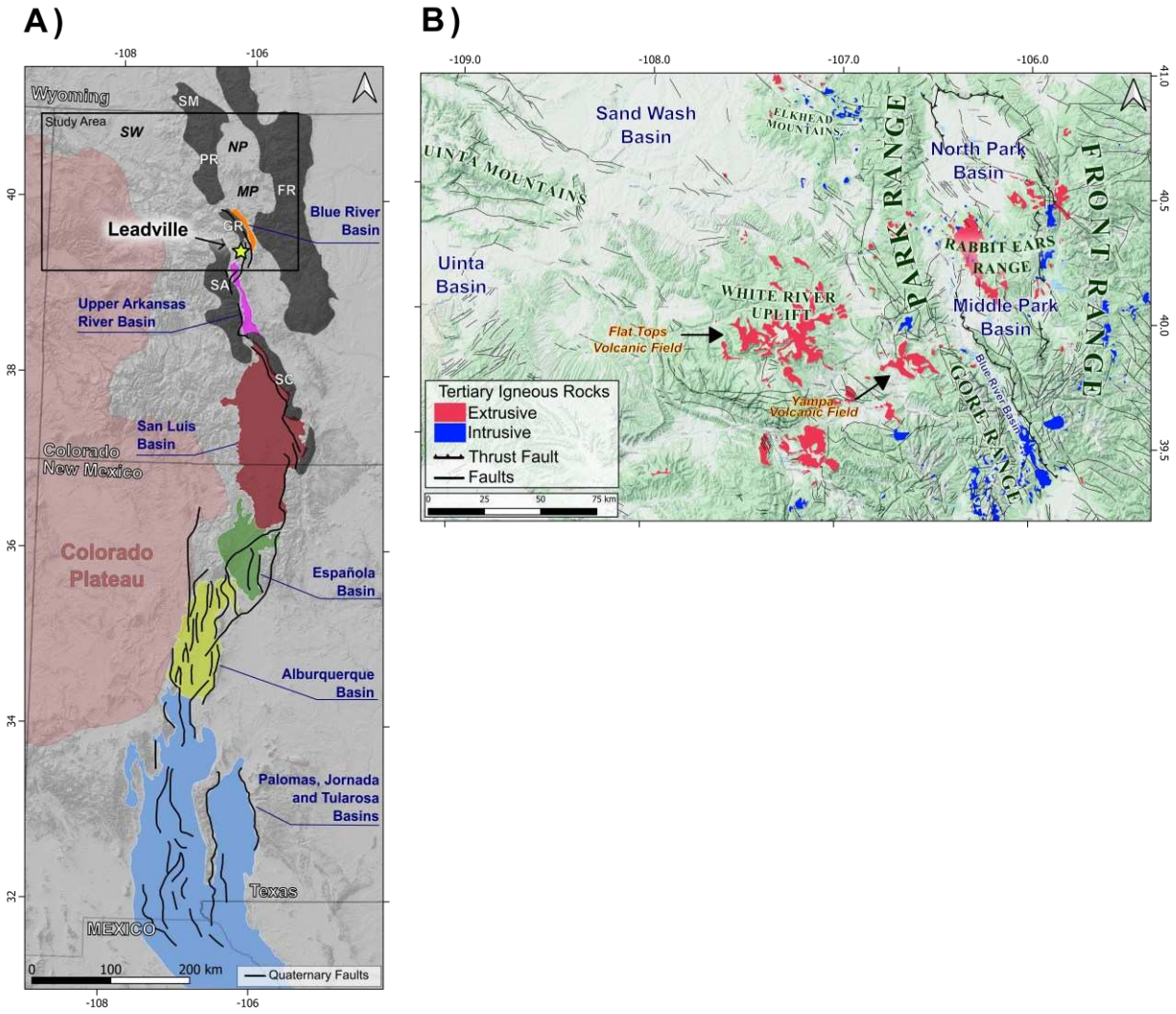

Figure 2: A) Rift basins forming the Rio Grande Rift. Laramide related uplifts in Colorado (Weil & Yonkee, 2023) are shown in dark grey and represent: SM - Sierra Madre; FR - Front Range; PR - Park Range; GR - Gore Range; SA - Sawatch Uplift; SC - Sangre de Cristo Range. Sedimentary basins in northwestern Colorado are: SW - Sand Wash Basin; NP - North Park Basin; MP - Middle Park Basin. Quaternary faults were obtained from (Abbey & Niemi, 2020). Black box outlines study area of this thesis. B) Study area in northern and northwestern Colorado showing main geographical and geological features. Faults and outcropping tertiary igneous rocks are shown from (Tweto, 1976).

The Upper Arkansas River Basin is located in central Colorado and its northern termination lays in the vicinity of the city of Leadville, where the physiographic expression of the rift ends (***Figure 1***). However, extensional features extend further north throughout north-central and northwest Colorado to the southern edge of the Wyoming craton near the Wyoming state border (Chapin & Cather, 1994). This

suggests that RGR-related extension might have developed further north than Leadville. This thesis focuses on the region north of the Upper Arkansas River Basin and Blue River Basin in north-central and northwestern Colorado. In this region, evidence of extensional features includes late Cenozoic faulting, sedimentary strata filling shallow extensional basins, and minor volcanism distributed throughout northwestern Colorado which coincide roughly in age with RGR development further south.

The region located immediately further north than the northernmost RGR rift basins remains an area where insufficient research has been done to evaluate possible RGR related extension. In this region sedimentary basins such as the Middle Park, North Park and Sand Wash Basin can be found. The Middle and North Park Basins lie between the Front Range to the east and the Park Range to the west, with both ranges being formed during a previous late Mesozoic and early Cenozoic Laramide orogenic period (Weil & Yonkee, 2023). The Sand Wash Basin is located west of the Park Range and extends westward to the Utah border and northwestward through southern Wyoming. Late Tertiary intermediate to mafic volcanic features exist in this region such as the Rabbit Ears Range, a volcanic complex between the Middle Park and North Park Basins. Smaller late Tertiary volcanic features and normal faulting can also be found extending west throughout the Sand Wash Basin to the edge of the Basin and Range Province near the Utah border.

The main hypothesis evaluated with this work is that extensional processes related to RGR rifting can be found in northern and northwestern Colorado, where the Middle and North Park Basins are located. To evaluate if RGR related extension is present further north than Leadville, previously collected gravity data in Colorado was complemented with newly collected gravity measurements. The data, combined with constraints from regional seismic observations, is used to construct forward gravity models that constrain the lithospheric and upper asthenosphere structure in the Middle/North Park and Sand Wash Basin regions, with the objective of assessing the pattern of lithospheric and crustal thinning that occurred in the area.

2. GEOLOGICAL BACKGROUND

RGR extension initiated contemporaneously across its entire length at approximately 25 Ma closely following the termination of the Laramide orogeny that dominated across western North America from the Late Cretaceous to the Eocene (Abbey & Niemi, 2018, 2020). Compressional stress in western North America during the Laramide orogeny was the result of the flat slab subduction during the Farallon-North American plate convergence (Weil & Yonkee, 2023). This produced a series of basement-cored uplifts bounded by reverse faults (***Figure* 2**). These uplifts can be found in Wyoming, Colorado, New Mexico and Arizona defining the Laramide deformation. In Colorado, the Laramide related uplifts are cored by Proterozoic basement rocks and in many places their uplifting reactivated prior Paleozoic structures related to the Ancestral Rockies. Important examples of these basement uplifted blocks include the Front Range, Park Range and the Sangre de Cristo arches (***Figure 2a***) (Weil & Yonkee, 2023).

During the late Oligocene, the mid-ocean ridge separating the Pacific and Farallon plates began to approach the western North American margin which resulted in the Farallon plate being progressively consumed in the convergent margin. Following the subduction of the Farallon ridge, this convergent margin was progressively replaced by a dextral transform boundary that grew between the Pacific and North American plates (The San Andreas fault system) (***Figure 1***) (Eaton, 2013). This caused a change in the regional stress field controlling deformation in western north America and induced westward extension in the Basin and Range region east of the growing transform boundary (Eaton, 2013). This led to the clockwise rotation of the Colorado Plateau as a discrete crustal block, which led to the onset of extension between the Colorado Plateau and the great Planes which opened the RGR (Chapin & Cather, 1994; Livaccari, 1979).

However, recent studies dispute the rigid-body rotation of the Colorado Plateau. GPS observations suggest instead that relative movement between the Colorado Plateau and the North American continent can be better characterized as diffuse in the RGR and New Mexico-Arizona region with significant east-west extensional deformation along the edges of the Colorado Plateau (Kreemer et al., 2010; Murray et al.,

2019). Additionally, the rotation of the Colorado Plateau cannot easily explain RGR related extension both in NW Colorado and in its southernmost basins located in New Mexico as these two areas extend beyond the north and south extent of the Colorado Plateau respectively. This points to the relationship between the Colorado Plateau and the opening of the RGR being more complex thus requiring the consideration of more factors to fully explain the onset of extension.

Additional available geodynamical models exist to account for the transition from Laramide compression to late Tertiary extension in the RGR, however a comprehensive set of mechanisms that led to the onset of extension has not been determined yet. Different explanations attempt to account for a change in the force balance acting on the western north American continent. In these models the Farallon slab generally plays an important role. During the late stages of the Laramide Orogeny, early extension in the RGR would have begun when the Farallon plate experienced slab rollback which was followed by extension and voluminous magmatism in Colorado and western North America during the Ignimbrite Flareup (Weil & Yonkee, 2023).

Possible contributing factors in the opening of the RGR include Mantle-Lithosphere interactions such as large-scale convection within the mantle below southwestern North America (Moucha et al., 2008) or small-scale convection aided by changes in lithospheric thickness with upwelling of hot material weakening the lithosphere in the RGR region (Van Wijk et al., 2008). Ricketts et al., (2016) proposed that tearing and foundering of decoupled portions of the Farallon slab would have focused convection and mantle upwelling in the N-S region where the RGR is now. This would have been caused by the Farallon slab encountering the thicker lithosphere of the Wyoming craton and great plains. Thus, the onset of RGR extension would have been driven by asthenosphere upwelling aided by thermal weakening of the lithosphere. Other contributing mechanisms include the collapse of overthickened crust in the Rocky Mountain region after the Laramide Orogeny compressive stress ceased. This would have been accompanied with increased lithospheric buoyancy due to basaltic and bimodal magmatism caused by the

rollback of the Farallon slab and the exposure of hydrated lithospheric mantle to the asthenosphere (Cather et al., 2012; Ricketts et al., 2016).

When extension initiated in the RGR, it exploited existing crustal weaknesses left by the Laramide related episode of shortening. This is evidenced by several rift basins in the RGR being bounded by reverse faults that were reactivated as normal, accommodating RGR related extension (Kellogg, 1999). Examples of these reactivated Laramide faults in the northern RGR can be found in the Sawatch Range and Gore Range which represent the western boundary of the Upper Arkansas River Basin and Blue River Basin respectively (***Figure 2***). Thermal history modelling indicates late Oligocene and early Miocene exhumation and cooling in the Sawatch Range fault bounding the Upper Arkansas River Basin and Miocene cooling in the Gore Range fault bounding the Blue River Basin (Abbey & Niemi, 2020; Ricketts et al., 2016).

Similar cooling histories are shown by thermochronology constraints for the RGR basins located further south, clearly indicating that normal fault displacement was contemporaneous along the entire length of the rift, south of the Blue River Basin (Abbey & Niemi, 2018, 2020; Landman & Flowers, 2013; Ricketts et al., 2016). Overall, thermal history analyses for the RGR suggest that extension on the RGR basins was accommodated through a process of fault initiation, lateral growth along strike, and ultimate linkage of the main RGR basin bounding faults through transverse accommodation zones. Additional extension between basins was then accompanied by transverse deformation within the accommodation zones which facilitated strain transfer and basin integration (Abbey & Niemi, 2020).

The current RGR system or RGR proper refers to the set of rift basins that opened due to RGR related late tertiary normal fault development and have associated deep tertiary sedimentary fill (***Figure 2a***). In this manner, the RGR basin system can be subdivided into the North, Middle and South RGR with extension decreasing towards the north. The physiographic RGR is segmented and most of its extensional basins are characterized by their asymmetry. The different RGR segments are defined by basins which are controlled by a north striking half graben that alternates from east to west tilted. Furthermore, the half

graben tilt reverses across accommodation zones which separate each segment of the RGR. (Chapin & Cather, 1994; Kellogg, 1999; Russell & Snelson, 1994).

The south RGR includes the Palomas, Jornada and Tularosa Basins located in southern New Mexico (***Figure 2a***). These are north-south oriented parallel basins. Horizontal extension in the southern RGR is the highest with estimates of up 50-100% of extension (Abbey & Niemi, 2020; Chapin & Cather, 1994; Morgan et al., 1986). The central RGR includes the southern and north Albuquerque Basins and the Española Basin in northern New Mexico (***Figure 2a***). Horizontal extension estimates vary from 28% in the Southern Albuquerque Basin to 17% in the northern Albuquerque Basin (Russell & Snelson, 1994). The Española Basin´s extension has not been estimated yet (Abbey & Niemi, 2020). The north RGR includes the San Luis Basin, Upper Arkansas River Basin and Blue River Basin with the Upper Arkansas River and Blue River Basins being located in the vicinity of the city of Leadville, where the physiographic expression of the RGR ends (***Figure 2a***). Estimates of horizontal extension in the San Luis Basin vary from 8-12% (Chapin & Cather, 1994) with no estimates available for the Upper Arkansas River Basin and Blue River Basin (Abbey & Niemi, 2020).

Assessing the full north and south extent of the RGR is a matter of debate and research. South of New Mexico, for example, discussion existed about whether the sedimentary basins that can be found south of the Alburquerque Basin (i.e. Paloma, Jornada and Tularosa Basins) are part of the RGR or if they cannot be distinguished from the Basin and Range province (Chapin & Cather, 1994). In this case, higher heat flow, late tertiary faulting and volcanism, and deep sedimentary fill would qualify this region as part of the RGR. However, the geophysical and structural signature associated with the RGR suggest that the extension mechanism might extend further south to include the Basin and Range west of Texas up to Chihuahua in Mexico (Seager & Morgan, 1979). Determining the northernmost extent of the RGR is similarly troublesome. The Upper Arkansas River Basin and the Blue River Basin are the northernmost recognized RGR basins as they display synchronous exhumation and cooling history in their basin-bounding faults as the other RGR basins in southern Colorado and New Mexico (Landman & Flowers, 2013). However,

isolated extensional basins which are structurally similar to the main rift basins of the RGR but lack deep tertiary sedimentary fill exist further north than the Blue Riven Basin, throughout north and northwest Colorado, central Wyoming and Northeastern Utah. Here, extension is more diffuse and broader with faulting and late tertiary volcanism that developed synchronously with the main RGR basins. (Chapin & Cather, 1994; Kellogg, 1999).

This thesis focuses on the northern and northwestern Colorado area just south of the Colorado-Wyoming state border and west of Fort Collins where sedimentary basins such as the Middle and North Park Basins, and the Sand Wash Basin are located (***Figure 2b***). The Middle and North Park Basins are bound by Laramide thrust faults that separate them, in the east from the Front Range which extends northward from central Colorado, and in the west from the Park Range which is located north of the Gore Range which in turn bounds the western side of the RGR Blue River Basin south of Middle Park (***Figure 2b***). Middle and North Park are also latitudinally separated by the Rabbit Ears Range, a volcanic complex. West of the Gore and Park Ranges there are low relief grabens with Miocene sedimentary fill extending up to Wyoming (Cosca et al., 2014). In this area, the Sand Wash Basin extends from northwest Colorado to southwest Wyoming. It is bounded on the east by the Park Range and Sierra Madre uplifts, and on the south by the White river uplift (Kaiser et al., 1992), to the southwest by the Uinta Uplift and to the northwest by the Rock Springs Uplift.

The northern Colorado region has a complex history shaped by sedimentation, volcanism and tectonic activity. In the late Mesozoic and early Cenozoic, the Laramide Front and Park Ranges were uplifted. This event marks the transition from late Cretaceous shallow marine sedimentary deposits associated with the Western Interior Seaway in North America, from which the Pierre Shale formation is the latest, to Tertiary and younger continental sedimentary deposits (***Figure 3a***). After the Front and Park Ranges were uplifted, the Paleocene Coalmont formation was deposited in the young Park Basins (Behrendt et al., 1969). During the Oligocene and Miocene, the White River, North Park and Troublesome formations were deposited and significant volcanic activity took place in the Rabbit Ears Range (Behrendt et al., 1969;

Raynolds & Hagadorn, 2017). Oligocene and Miocene volcanism in the Rabbit Ears comprises units of olivine- bearing trachybasalt flows overlaid by lavas of intermediate composition. The most recent volcanic unit is the Grouse Mountain Basalt of Pliocene age which contains olivine bearing basalt flows (***Figure 3b***) (Glen, 1966).

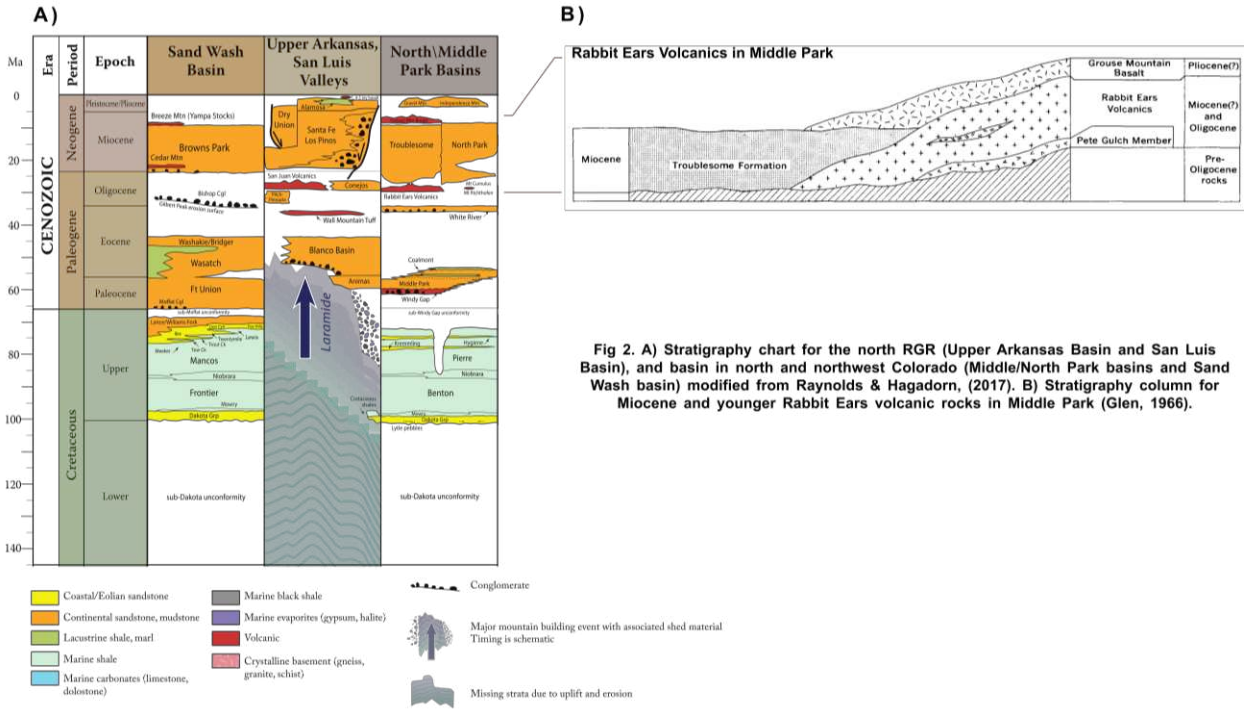

Fig 2. A) Stratigraphy chart for the north RGR (Upper Arkansas Basin and San Luis Basin), and basin in north and northwest Colorado (Middle/North Park basins and Sand Wash basin) modified from Raynolds & Hagadorn, (2017). B) Stratigraphy column for Miocene and younger Rabbit Ears volcanic rocks in Middle Park (Glen, 1966).

Figure 3: Stratigraphy chart for the northern RGR basins (Upper Arkansas Basin and San Luis Basin), and the basins located in northern and northwestern Colorado (Middle/North Park Basins and Sand Wash Basin) modified from (Raynolds & Hagadorn, 2017). B) Stratigraphy column for Miocene and younger Rabbit Ears Range volcanic rocks in Middle Park (Glen, 1966).

Volcanic activity becomes more diffuse west of the Park Range with small and scattered Pliocene and Miocene extrusive and intrusive igneous rocks of basaltic and intermediate composition (***Figure 2b***) (Tweto, 1976). Volcanic fields west of the Park Range include the Flat Tops, Elkhead Mountains and the Yampa volcanic field (Cosca et al., 2014). In the Yampa volcanic field, alkaline and mafic lavas have major and trace element geochemical signatures that are characteristic of the early stages of continental rifting and with studies of mafic magmas in NW Colorado, suggest that these rocks originate from partial melt in

subcontinental lithospheric mantle or asthenosphere mantle. This indicates that low degree extension exists in NW Colorado (Cosca et al., 2014; Gibson et al., 1992).

The RGR has been the subject of multiple geophysical studies to better characterize its extensional regime and structure. Both receiver function analysis and seismic refraction analyses show crustal thinning in the RGR area in comparison to the crust of the Great Planes and Colorado Plateau. The zone of crustal thinning widens as the RGR widens to the south (Keller & Baldridge, 1999). Crustal thickness estimates based on PdS and SdP receiver function analysis and Rayleigh wave tomography vary from approximately 40-53 km in the Colorado Plateau and southern Rocky Mountains, to ~45 km in the Great Planes area and ~35 km in the RGR region (Schmandt et al., 2015). Total lithosphere thickness in the RGR follows a similar trend showing thickening from ~75 km in the southern RGR to ~85 km in the northern RGR (Levander et al., 2011; Schmandt et al., 2015; Wilson et al., 2005). In Colorado, surface wave tomography analysis shows the lowest shear wave upper mantle velocity and shallowest Moho in the San Luis Basin region and the highest shear wave upper mantle velocity and deepest Moho located in northwest Colorado (***Figure 4***) (Hansen et al., 2013). Body-wave tomography indicates low shear wave velocity particularly in the upper mantle beneath central and south RGR at approximately 60-200 km which extends to surround the Colorado Plateau. This has been interpreted to denote a zone with possible low partial melt originating from the asthenosphere and mantle upwelling (Levander et al., 2011; Sosa et al., 2014). Low Vp in the crust beneath the Rift also suggest warming due to extension and lithospheric thinning (Keller & Baldridge, 1999).

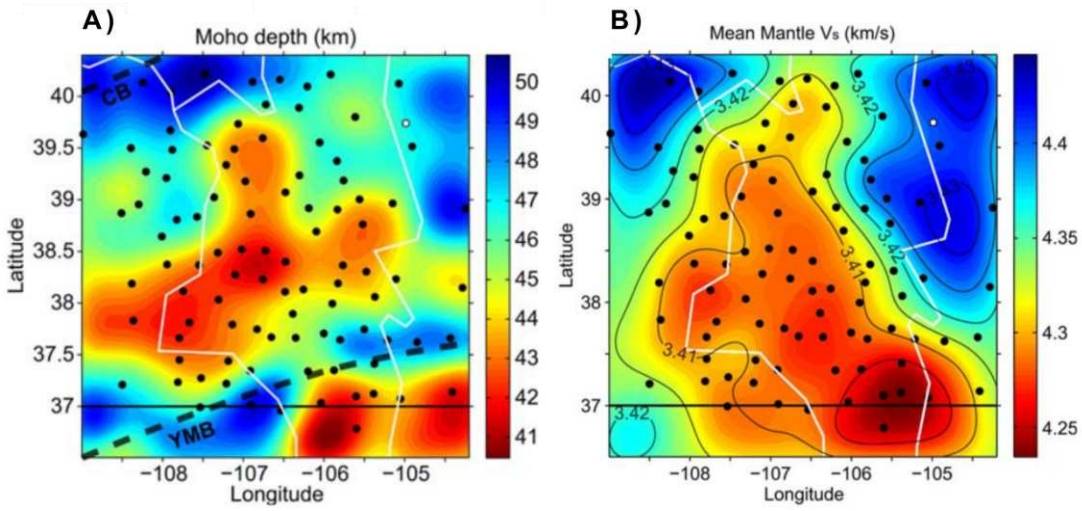

Figure 4: A) Crustal thickness map for Colorado derived from P-wave receiver function imaging. B) Mantle shear wave velocity from the Moho to 170 km depth obtained from surface wave tomography. Dashed lines indicate the Proterozoic crustal boundaries representing: CB-Cheyenne belt, YMB-Yavapai Mazatzal boundary. Black circles indicate station locations. White lines indicate the physiographic provinces in Colorado. Modified from (Hansen et al., 2013).

These regions of low velocity also coincide geographically with the location of major volcanic features on the flanks of the rift such as the San Juan volcanic field and volcanic trends that transect the rift such as the Jemez lineament (Ricketts et al., 2016). Additionally, three dimensional magnetotelluric imaging shows north-south oriented high conductivity tabular features near the base of the crust in the RGR area with pipe-like vertical extensions rising to the middle and upper crust. These features have been interpreted as signatures of volatiles released from stalled magmatic intrusions in the lower crust being introduced suggesting that the RGR is a tectonomagmatically active region (Murphy et al., 2024). Changes in lithospheric thickness have been attributed to Precambrian crustal boundaries associated with the Cheyenne belt suture zone between the Proterozoic Colorado crust and the Wyoming cratonic province in northern Colorado and the Yavapai-Mazatzal suture zone in southern Colorado. This suggest that structural inheritance in the lithosphere played an important role in RGR extensional evolutionary history (Abbey & Niemi, 2020; Hansen et al., 2013; Levander et al., 2011).

3. METHODS

3.1. Gravity Data

To test the hypothesis, a forward gravity model was constructed to constrain the lithospheric and upper asthenosphere density structure. The gravity data used originates from the PACES dataset (Keller et al., 2006) provided by Dr. Kevin Mickus of Southwest Missouri State University. This data was supplemented with 192 new gravity measurements that were collected for this thesis using a Scintrex CG5 gravity meter in the areas of diffuse volcanism west of the Park Range where the coverage in the PACES gravity dataset is sparse (***Figure 5***). The gravity field was measured over a five-day field campaign in July, 2024. Gravity measurements were collected, with a nominal spacing of 1.5 km, throughout the accessible roads west of the Park Range. A base station was repeatedly used each day to account for drift effects and reoccupied the day after to link all daily datasets (***Figure 5***).

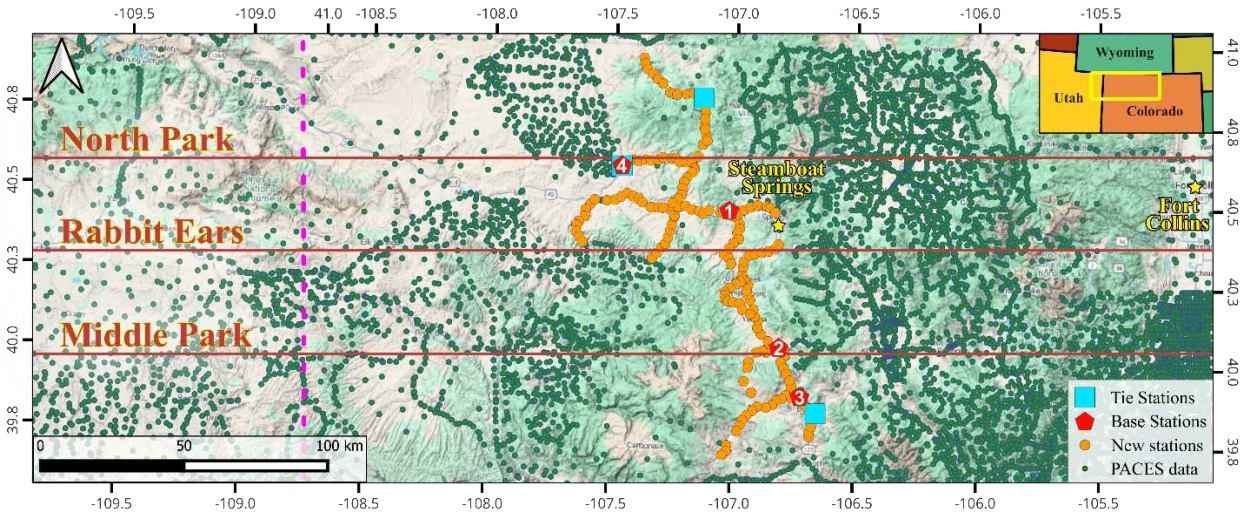

Figure 5: PACES and newly collected gravity data used for the research work done in this thesis. Base stations used during the gravity field campaign and tie stations used to integrate the PACES and new gravity measurements are included. The three E-W cross sections employed for the forward modelling are shown as red lines (Middle Park, Rabbit Ears Range and North Park cross sections). Receiver functions derived profile used to constrain the lithospheric mantle/lower crust boundary (Crosswhite & Humphreys, 2003) is shown as a dashed pink line.

The new gravity data was reduced following the gravity reduction procedure presented by (Hinze et al., 2005) with the objective of integrating this data into the PACES dataset. To tie the collected gravity data to the PACES data, the raw gravity measurements were corrected for instrument height, tidal effects and drift. The instrumental height correction was calculated using a free air gravity gradient of 0.3086 mGal/m. The tidal correction was calculated with LTide, a freely available MatLab tool to calculate tidal gravity effects (Bjelotomić Oršulić et al., 2019). After tide effects were removed, the gravity readings for each daily dataset were drift corrected by applying a linear fit to three base station measurements of the same day. Afterwards all daily datasets were tied to the base station of the first day (Base Station 1) (***Figure 5***) with the objective of integrating all data collected in the field. Finally, after the height, tide and drift corrections were applied, the corrected gravity values were tied to the PACES dataset. This was done by computing the average difference between the PACES data and the corrected gravity data that was collected during this survey. The average difference between the two stations was computed at three stations that were commonly located in the two surveys (***Figure 5***).

The integrated dataset was used to obtain the free air anomaly (FAA) at 5000m (***Figure 6***) by calculating the difference between the corrected observed gravity and the theoretical gravity value at each station location. First, the observed gravity and the theoretical gravity at each station were calculated by reducing the integrated dataset and the ellipsoidal gravity to a common datum at 5000 m by applying a free air correction in both cases.

$$Observed\ Gravity = Integrated\ Dataset + Free\ Air\ Correction\ (To\ 5000m)$$

$$Theoretical\ Gravity = Ellipsoidal\ Gravity + Free\ Air\ Correction\ (To\ 5000\ m)$$

The ellipsoidal gravity on the ellipsoidal surface is given by (Hinze et al., 2005).

$$g_t = \frac{g_e(1 + ksin^2(\varphi))}{(1 - e^2 sin^2(\varphi))^{1/2}}$$

Where g_e is the normal gravity value at the equator and with a value of 978032.67715 mGal; k is a derived constant equal to 0.001931851353; e^2 is the first numerical eccentricity squared and equal to 0.0066943800229 and φ is equal to the latitude of the gravity station.

The free air correction utilized corresponds to the second order approximation described by Hinze et al. (2005):

$$\delta g_h = -\big(0.3087691 - 0.0004398 sin^2(\varphi)\big)h + 7.2125\text{x}10^{-8}h^2$$

Where h is the altitude of the gravity station above the ellipsoid. The altitude of the gravity stations was obtained from the USGS 1/3 arc second elevation product derived from the USGS's 3D elevation program (3DEP) (U.S. Geological Survey, 2024).

Finally, the difference between the observed gravity and theoretical gravity was calculated with the following formula (Hinze et al., 2005):

$$FAA = Observed\ Gravity - Theoretical\ Gravity$$

To start the forward modelling process, the obtained FAA datapoints were used to create a grid using Golden Software's Surfer employing the Natural Neighbor method with a cell size of 1500x1500 m. This gridded data (***Figure 6***) was compared to the calculated anomaly during forward modeling.

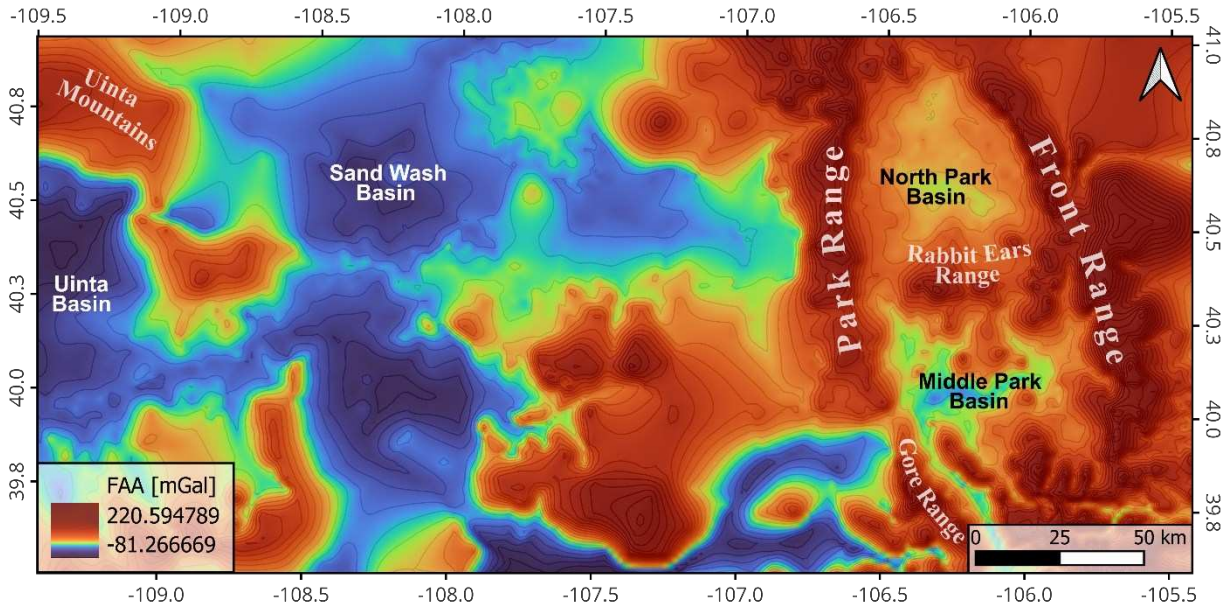

Figure 6: Free Air Anomaly (FAA) at 5000 m elevation used for forward modelling. Main physiographical features in the study area are included.

3.2. Forward Modelling

The 3D gravity modelling software IGMAS+ (Schmidt et al., 2007) was used to create the forward model. IGMAS+ works by triangulating a set of polyhedrons of homogenous density which in conjunction approximate the subsurface density configuration. The algorithm that calculates the total gravitational effect of the model is based on the conversion of the volume integral that yields the gravitational effect of any polyhedral into the sum of line integrals that yield the gravitational effect of its individual bounding surfaces. This allows the fast calculation of gravity effects (Götze & Lahmeyer, 1988).

The model is constrained by setting the density distribution configuration in parallel vertical 2D profiles where all the model elements are configured (***Figure 7***). IGMAS+ then interpolates the density model between the parallel profiles to create the 3D density distribution model. This model is triangulated as described above and used to calculate the modelled gravity. The modelled gravity was set to be calculated at 5000 m above sea level concurrent with the FAA datum. For the study area of this thesis, the forward model was configured with three east-west oriented cross sections that cut the North Park Basin, the Rabbit Ears Mountain and Middle Park Basin (***Figure 5,7***). All structural profiles extend from the Front Range in

the east to 1 degree west past the Utah-Colorado state border. Additionally, the model extends to a depth of 150 km to constrain density structure in the lithosphere as well as the upper asthenosphere. Both the North Park Basin and Middle Park Basin cross sections represent the northern and southern edge of the 3D density structure.

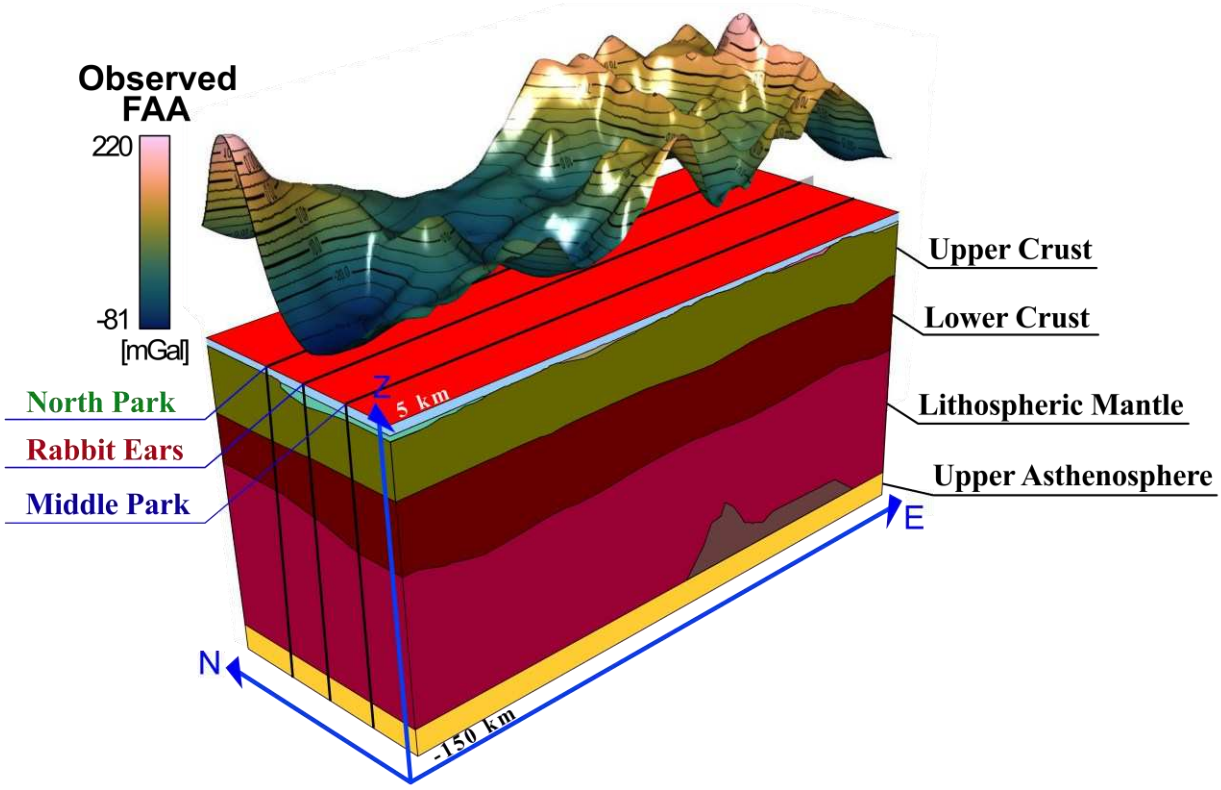

Figure 7: Setup of the density structure in IGMAS+ during the forward modelling process.

The focus of this study is to constrain the large-scale density structure of the crust and lithosphere. Therefore, the primary focus of the modelling was to match wavelengths in the gravity field longer than 20 km. The general layered lithosphere structure used as a starting point for the forward modelling process was modified from (Abdullin, 2012), who employed gravity spectral analysis to estimate the depth to the

main lithospheric density contrasts in the region. This layered structure includes a felsic upper crust, a more mafic lower crust, and an ultramafic lithospheric mantle and upper asthenosphere (***Figure 7***).

The study area spanned five major sedimentary basins: The Denver Basin, the Park Basins (Middle and North Park), the Sand Wash Basin and the Uinta Basin (***Figure 5***). Sedimentary basin depth in the study area was constrained from existing structural maps. Depth to the Denver Basin sedimentary basement was constrained from the Precambrian basement depth map for the state of Colorado (Hemborg, 1996). The sedimentary depth in the Sand Wash Basin was constrained from the structure contour map of the top of the Dakota Sandstone for the greater Green River Basin for Wyoming, Colorado and Utah (Lickus & Law, 1988). The sedimentary depth for the Middle and North Park Basins was constrained from the crystalline basement structure contour map for these basins (Behrendt & Popenoe, 1969). The sedimentary depth of the Uinta Basin was constrained from the structure contour map of the top of the Dakota sandstone for the Uinta-Piceance province (Roberts, 2003).

The lithospheric mantle/lower crust boundary was constrained from two main datasets: A gridded crustal thickness map from USArray receiver function analyses (Schmandt et al., 2015) and a local receiver function derived profile from the Deep Probe and Lodore seismic arrays (Crosswhite & Humphreys, 2003). During the forward modelling process, the sedimentary basin basement depth and the base of the crust were treated as fixed boundaries. The other layer boundaries in the density forward model that were not constrained from other studies were iteratively modified to improve the misfit between the calculated and observed gravity anomaly.

4. RESULTS

Figure 8 shows the simplest lithosphere/asthenosphere layered model which represents the starting point for the forward modelling process. The model shows the east-west oriented cross sections that cut Middle Park, the Rabbit Ears Range and North Park and includes relief only on the lithospheric mantle/lower crust boundary with constraints derived from receiver functions (Crosswhite & Humphreys, 2003; Schmandt et al., 2015). This model layout is modified from the basic layered structure from (Abdullin, 2012). The Abdullin (2012) model has an upper crust of 2.761 g/cm^3, a lower crust of 2.968 g/cm^3, a lithospheric mantle of 3.28 g/cm^3 and a upper asthenosphere divided into a western asthenosphere of 3.3 g/cm^3 and an eastern asthenosphere of 3.31 g/cm^3. The average depths to the base of the upper crust, lower crust and lithospheric mantle in the Abdullin (2012) model are 21.5 km, 48.9 km and 100 km respectively.

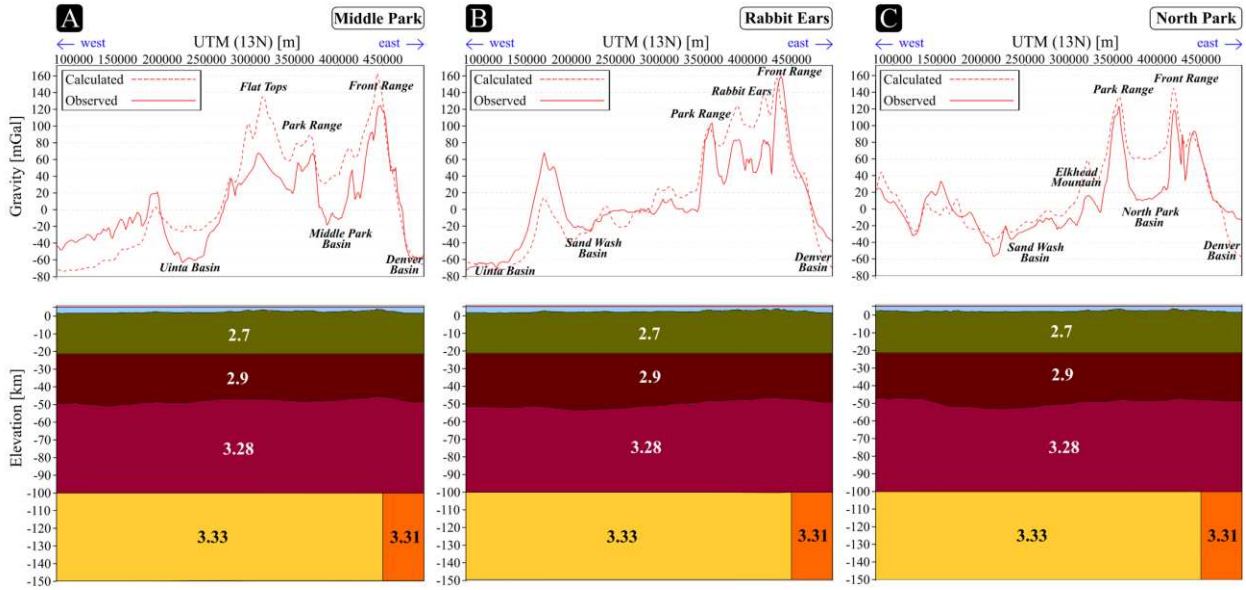

Figure 8: Simplest lithosphere/asthenosphere layered forward model including only constraints for the lithospheric mantle/lower crust boundary (Crosswhite & Humphreys, 2003; Schmandt et al., 2015). Cross section locations can be found in Figure 5.

From this model the upper crust density was modified to have a density of 2.7 g/cm^3 to represent a felsic upper crust. This corresponds to the Precambrian basement in northern Colorado. These rocks are heavily metamorphosed and present granitic rocks, schists, gneisses and, gabbroic and diabase mafic intrusive rocks (Tweto, 1976). The lower crust was also modified to have a density of 2.9 g/cm^3 representing a mafic composition. Changing these densities improved the long and short wavelength effect of the additional igneous and crustal density features in the final density forward model (***Figure 11***) allowing a better gravity anomaly fit.

The lithospheric mantle and upper asthenosphere densities (3.28 g/cm^3 and 3.3 g/cm^3, 3.31 g/cm^3 respectively) were not modified. Abdullin (2012) derived these densities from seismic velocities in the lithosphere and mantle (Rumpfhuber & Keller, 2009) employing the velocity-density equation from (Brocher, 2005). The base of the lower crust is shallowest in the Park Basins region for all cross sections (***Figure 8***), reaching ~46 km in the Front Range area, and it is deeper towards the western edge of the study area in the Middle Park and Rabbit Ears Range cross sections (***Figure 8a,b***), near the Colorado-Utah state border and Uinta Basin reaching ~53 km deep.

(***Figure 9,10,11***) show progressively more complex models in order to highlight how the different elements of the lithosphere and upper asthenosphere in the finished forward model (***Figure 11***), which shows the complete density structure, affect the difference between the calculated and observed anomaly for the study area. ***Figure 9*** shows the layered model from ***Figure 8*** with additional constraints for sedimentary basins (Behrendt & Popenoe, 1969; Hemborg, 1996; Lickus & Law, 1988; Roberts, 2003), and after iteratively modifying the base of the upper crust.

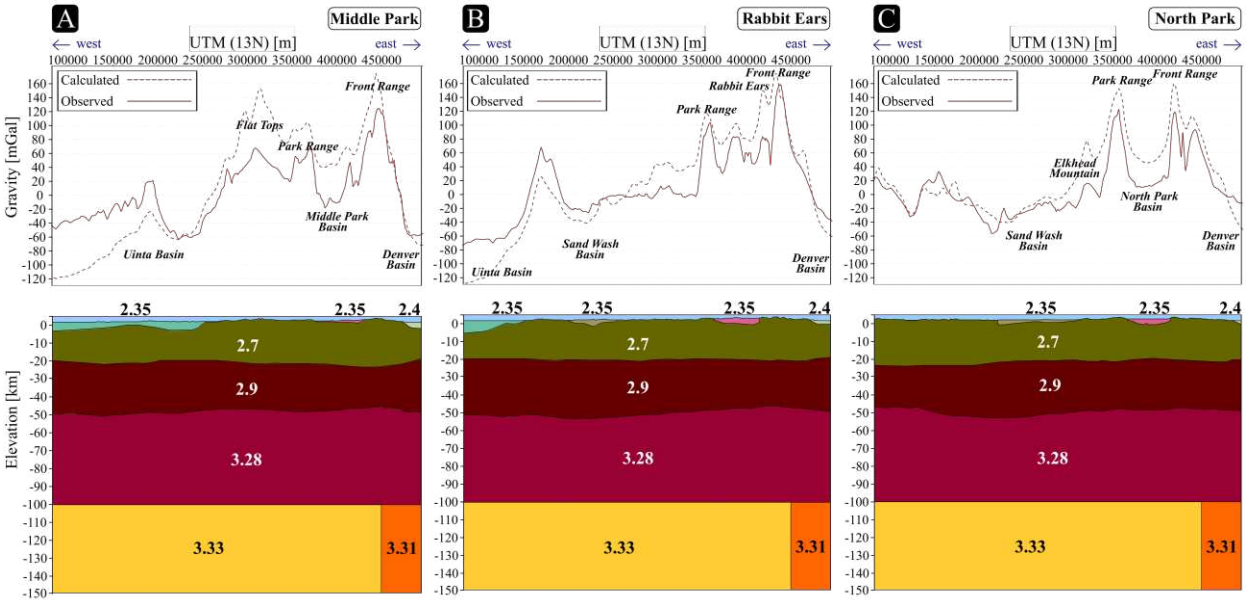

Figure 9: Forward model including constraints for basin sedimentary depth (Behrendt & Popenoe, 1969; Hemborg, 1996; Lickus & Law, 1988; Roberts, 2003) and modification of the upper crust. Cross section locations can be found in Figure 5.

The sedimentary basins in the model are shown to have a considerable long wavelength effect, lowering the calculated gravity anomaly estimation over the sedimentary basins (***Figure 9***). The Uinta Basin, Sand Wash Basin and Park Basins structural maps employ early and late Mesozoic datums to define the base of the sediments (Behrendt & Popenoe, 1969; Lickus & Law, 1988; Roberts, 2003) . Sedimentary rocks in these basins, which are Mesozoic and younger in age, include continental and marine shales, sandstones and mudstones (Raynolds & Hagadorn, 2017) for which an average density of 2.35 g/cm^3 was used. The Denver Basin was constrained from a structural map using the deeper Precambrian basement as a datum for the basin basement. Sedimentary rocks in this basin, which are Paleozoic and younger in age, include continental and marine sandstones, shales, mudstones and carbonates for which an average density of 2.4 g/cm^3 was used.

The depth to the base of the upper crust was modified to better fit the long wavelength gravity anomaly misfit at the edges of the study area in the final model (***Figure 11***) over the Denver Basin and in the Colorado-Utah state boundary. In all cross sections, the base of the upper crust was shallowed to ~17 km in the Middle Park cross section, ~19 km in the Rabbit Ears Range cross section and ~15 km in the

North Park cross section. This thinned the upper crust in the Denver Basin region (***Figure 9a,b,c***) and improved the fit of the gravity anomaly underestimation in this area. The base of the upper crust deepens to ~21.7 km thickening this layer west of the Denver Basin in all cross sections (***Figure 9a,b,c***). And in the North Park cross section (***Figure 9c***), the base of the upper crust was further deepened to 23.5 km to accommodate the long wavelength overestimation near the Colorado-Wyoming border.

The calculated anomaly behavior in ***Figure 9*** clearly shows that this basic layered model produces a gravity anomaly overestimation towards the eastern end of the study area, over the Front Range, Park Basins and Park Range. Additionally, a gravity anomaly underestimation is observed in the western end of the study area (***Figure 9***), over the Uinta and Sand Wash Basins, west of the Park Range. Moreover, ***Figure 9*** shows that the contrast between the gravity anomaly overestimation and underestimation for each cross section becomes more pronounced towards the south. In the Middle Park Basin profile (***Figure 9a***), the positive misfit is the highest and extends over the Park Range and Flat Tops, Middle Park Basin and the Front Range reaching ~90 mGal over the Park Range and Flat Tops. The negative misfit reaches ~80 mGal in the Uinta Basin region. In the Rabbit Ears Range profile (***Figure 9b***) the positive misfit reaches ~40 mGal west of the Park Range and it decreases over the Rabbit Ears Range. The negative misfit reaches ~60 mGal in the Uinta Basin region. In the North Park profile (***Figure 9c***) the positive misfit is located mostly over the North Park Basin and west of the Park Range reaching ~60 mGal west of the Park Range and ~50 mGal in the North Park area. The negative misfit reaches ~20 mGal on the western side of the Sand Wash Basin.

To better replicate the observed gravity anomaly, the density of the lithosphere in the Park Basins region was reduced by adding igneous intrusions (***Figure 10***). The forward modelling process showed that these igneous features needed to be distributed at different depths within the lithosphere. Igneous features were first added at the base of the lithosphere to accommodate the long wavelength component of the gravity anomaly in the Park Basins region in all cross sections. To accommodate the shorter wavelength

component of the gravity anomaly, additional igneous features were added in shallower locations, at the base of the lower crust and the base of the upper crust.

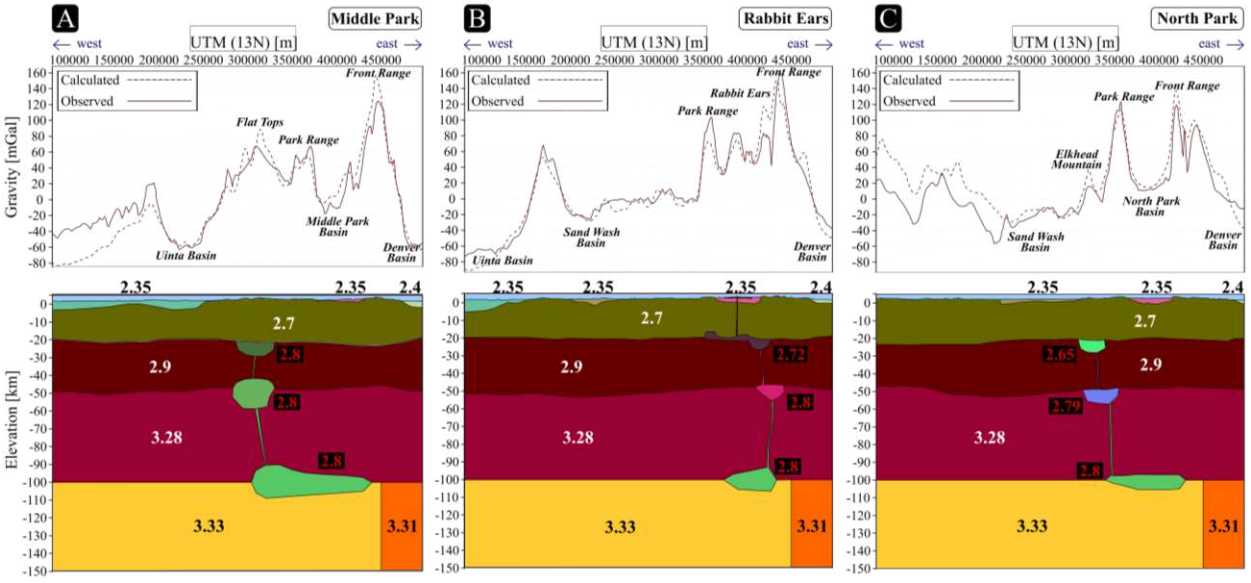

Figure 10: Forward model including igneous features at the base of the upper crust, lower crust and base of the lithosphere. Cross section locations can be found in Figure 5.

In the Middle Park cross section (***Figure 10a***) the long wavelength component of the gravity anomaly overestimation in the Middle Park Basin, Park Range and Front Range was accommodated by adding a mafic igneous body at the base of the lithosphere with a density of 2.8 g/cm^3. The short wavelength component of the gravity anomaly positive misfit is located west of the Middle Park Basin over the Flat Tops (***Figure 10a***). This region is characterized by surface outcrops showing widespread dense basalts and resistant lava rocks (Tweto, 1976). This misfit was accommodated by adding two mafic igneous bodies with a density of 2.8 g/cm^3 at the base of the lower crust and base of the upper crust.

For the Rabbit Ears Range cross section (***Figure 10b***), the long wavelength component of the gravity anomaly overestimation over the Rabbit Ears Range and west of the Park Range was accommodated by extending the 2.8 g/cm^3 mafic igneous body at the base of the Middle Park cross section lithosphere (***Figure 10a***) to the Rabbit Ears Range cross section. This igneous body has a smaller cross-sectional area

at the Rabbit Ears Range cross section in comparison to the Middle Park cross section. The short wavelength component of the gravity anomaly positive misfit is located over the Rabbit Ears Range volcanics and Front Range area (***Figure 10b***). This misfit was improved by adding mafic igneous bodies of 2.8 g/cm^3 at the base of the lower crust and 2.72 g/cm^3 at the base of the upper crust. These igneous rocks extend to the surface and outcrop at the Rabbit Ears Range.

For the North Park Basin cross section (***Figure 10c***), the 2.8 g/cm^3 mafic igneous body at the base of the lithosphere was extended further north from the Middle Park and Rabbit Ears cross sections to accommodate the long wavelength component of the positive gravity anomaly misfit in North Park Basin. The short wavelength component of the anomaly misfit is located west of the Park Range over the Elkhead Mountains region (***Figure 10c***). This region is characterized by discrete outcrops of intermediate and basaltic intrusive porphyritic rocks and intermediate volcanic compositions (Tweto, 1976). This misfit was improved by adding a mafic igneous body of 2.79 g/cm^3 at the base of the lower crust and a felsic igneous body of 2.65 g/cm^3 at the base of the upper crust.

The gravity anomaly misfit over the Sand Wash and Uinta Basins remained after improving the density forward model in the Park Basins region (***Figure 10***). This misfit was further improved by considering lateral changes in the lithosphere's nature west of the study area near the Utah-Colorado and Wyoming-Colorado state border. Lithospheric structure in this region is influenced by the northeast trending suture zone that separates the Proterozoic Yavapai terrains which occupy the state of Colorado and the North American Archean crust of the Wyoming Craton in Utah (Whitmeyer & Karlstrom, 2007). Additionally, near the northwestern Colorado-Wyoming state border, the Cheyenne suture zone defines the transition from the Proterozoic Yavapai terrains of Colorado and the Wyoming archean cratonic province in the North (Whitmeyer & Karlstrom, 2007).

To account for these changes in lithospheric structure, the upper crust was divided to introduce a denser upper crust west of the Park Range (***Figure 11***). The density of the western upper crust was iteratively changed until achieving a reasonable fit between the observed and calculated gravity anomaly.

In the Middle Park Basin cross section (***Figure 11a***), a western upper crust with a density of 2.75 g/cm^3 was used. In the Rabbit Ears Range cross section (***Figure 11b***), a western upper crust with a density of 2.72 g/cm^3 was used. In the North Park Basin cross section, a western upper crust of 2.71 g/cm^3 and a western lower crust with a density of 2.83 g/cm^3 was used to define the transition to the Wyoming cratonic province.

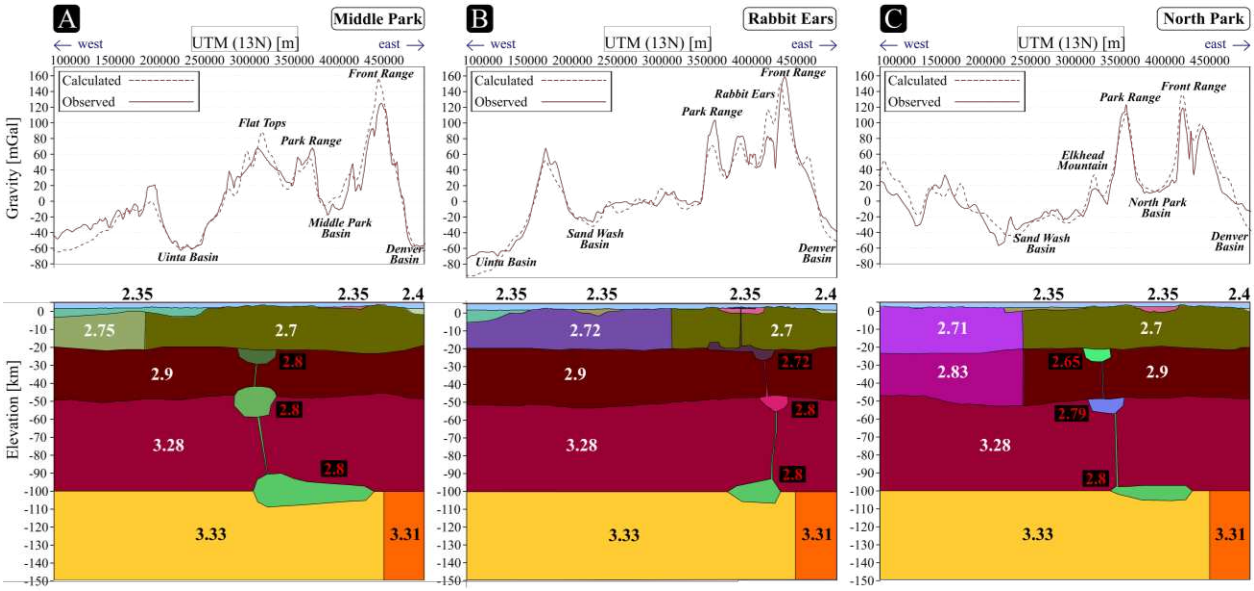

Figure 11: Complete forward model including lateral density variations within the lithosphere. Cross section locations can be found in Figure 5.

As shown by the complete density forward model (***Figure 11***). The long and short wavelength components of the gravity field were best fit with a relatively simple layered model. The long wavelength components of the gravity anomaly misfit towards the western end of the study area were fitted with lateral density changes in the crust and a thinned upper crust. In the Park Basins region, towards the eastern end of the study area, the long wavelength components of the gravity anomaly were fitted with a mafic igneous body at the base of the lithosphere. The short wavelength component of the gravity anomaly misfit was fitted by including igneous bodies at the base of the upper crust and lower crust. The final model (***Figure***

11) shows that less voluminous and more felsic rocks are required in the lithosphere towards the north of the study area in order to better replicate the observed gravity anomaly.

5. DISCUSSION

The results of the gravity forward model (***Figure 11***) allow us to make important interpretations about the lithospheric structure and how extension is accommodated throughout the lithosphere over the Park Basins region in north central and northwest Colorado. The forward modelling results (***Figure 11***) provide valuable constraints on the location, volume, and composition of intrusive igneous rocks and how they vary from south to north in the study area.

5.1. Model Uncertainty

It is important to note that the solution obtained from forward gravity modelling (***Figure 11***) is non-unique and alternative or modified density distributions and configurations that differ from the models presented here may produce a similar gravity anomaly fit. For example, the short wavelength component of the gravity anomaly misfit has been accommodated by adding intrusions that become progressively more felsic in the lower and upper crust northward from Middle Park, through the Rabbit Ears, and into North Park. These more felsic igneous densities could be raised if the cross-sectional area of these intrusives are increased, replacing the denser surrounding crustal rocks. This also results in a reduction of the gravity anomaly overestimation. However, these larger igneous bodies increased the long wavelength effect of these features, worsening the gravity anomaly fit in the area. Additionally, alternative forward models attempted to accommodate the gravity anomaly misfit with lateral density variations within the crust, which would imply east-west changes in crustal composition. However, this configuration resulted in an overly complex density structure with unreasonable low crustal densities which were required to accommodate the short wavelength component of the gravity anomaly misfit.

Given these limitations, the simpler model presented here was preferred as it did not introduce considerable complexity which could result in an unrealistic structural representation. Thus, the forward modelling process showed that the most reasonable density forward model for the study area covered in this work requires igneous rocks at depth the locations indicated in the models. The igneous bodies vary in

volume and composition from south to north, with less dense (or felsic) igneous compositions towards North Park in comparison to Middle Park. The following discussion addresses the spatial extent and distribution of these density features in the lithosphere and how they vary throughout the study area.

5.2. Model Implications

The results show that the volume and lateral extent of the igneous rocks required to be present in the lithosphere to accommodate the gravity anomaly in the Park Basins region decreases toward the north with the most voluminous magmatic intrusive rocks being present in the Middle Park lithosphere and the least voluminous magmatic intrusive rocks being present in the North Park Basin region. Generally, magmatism in extensional systems is associated with decompression melting, with greater amounts of extension leading to more decompression and thus more magmatism (Mayle & Harry, 2023). The presence of a complex pattern of igneous intrusions present in the crust and lithospheric mantle across the corridor defined by the Middle Park, Rabbit Ears Range and North Park (***Figure 11***) suggest that lithospheric thinning is present in the Park Basins region with more extension being accommodated in the Middle Park Basin region than in the North Park Basin region which correlates with RGR extension being more developed towards the south.

This lithosphere extensional corridor with igneous intrusions beneath Middle Park, Rabbit Ears Range and North Park corelates with P-wave receiver function derived Moho depths showing a N-S trend of shallow mantle beneath the main RGR rift basins further south that extends into northern Colorado, reaching ~47 km in the Middle Park Basin region (Hansen et al., 2013). Furthermore, the gravity models correlate with estimations of lithosphere-asthenosphere boundary (LAB) depths derived from PdS and SdP receiver functions and Rayleigh wave inversion showing a broad area of LAB shallowing in the Park Basins area in northern Colorado (~95 km to ~105 km) (Levander et al., 2011). Estimated seismic velocities also show a zone of low Vs in the middle and lower crust (Schmandt et al., 2015) and a zone of low Vs and Vp at 80 km of depth (Levander et al., 2011), both of which follow the RGR latitudinal extent in northern New Mexico and southern Colorado. This trend of low Vp and Vs velocities extends further north than central

Colorado into southern Wyoming, covering the Middle and North Park Basin region. Shallowing of the LAB and Moho depth, together with a reduction of Vp and Vs seismic velocities and the results of the gravity forward modelling indicating the presence of a low density anomaly at the base of the lithosphere in the Park Basins region (***Figure 11***) indicates that this region may be an area where decompression melting has occurred.

The mafic igneous rocks present at the base of the lithosphere in the final forward model (***Figure 11***) can be interpreted as synrift magmatic intrusions produced from partial melting of a fertile source within the lithosphere mantle and/or upper asthenosphere. Several geodynamic analyses indicate that syn-rift magmas may originate after only minor amounts of extension due to decompression melting of hydrous and compositionally fertile mafic sources that produce high melting rates at the onset of extension. These sources can exist if the lithosphere or asthenosphere mantle has been hydrated, intruded or replaced by distinct materials emplaced prior to rifting. Such sources may take the form of mafic or ultramafic dikes, slab remnants, intrusive bodies, or pervasive hydration and/or metamorphism (Mayle & Harry, 2023). Thus, the igneous bodies present at the base of the lithosphere in the forward model (***Figure 11***) would have originated from partial melting of these fertile sources required to produce synrift intrusives in the Park Basins region without a considerable amount of extension.

These fertile magmatic sources are possible to originate from lithosphere-asthenosphere interactions beneath the Middle and North Park Basin region during the late stages of the Laramide orogenic period. Tearing and foundering of the Farallon slab during its descent into the asthenosphere, after interacting with the thickened lithosphere in the Wyoming craton region (Ricketts et al., 2016), could have provided fertile sources favoring partial melting. Therefore, the most likely explanation for the igneous rocks present at the base of the lithosphere in the study area is that the prior history of subduction in the Colorado state area played an important role by placing fertile intrusions in the lithospheric mantle and possibly the asthenosphere. These fertile materials then began to undergo partial melting despite minimal tectonic extension. In this context, the latitudinal composition variation in the composition of the igneous

rocks (***Figure 11***) present in the forward model upper and lower crust may reflect either more advanced degrees of magmatic differentiation during ascent through the lithosphere or lesser partial melting towards the North Park Basin region, where extension is less developed than in the Middle Park region.

Additional consideration should be given to the discrepancy between the expression of extension throughout the depth of the lithosphere present in the Park Basins region and the lack of localized extension in the surface similar to the main RGR rift basins found further south. Previous three-dimensional magnetotelluric imaging in the northern RGR located in central Colorado, and south of Middle Park, has mapped high conductivity tracks in the lower and upper crust which extend longitudinally past the surface expression of RGR rifting, suggesting that RGR related processes in this region are acting on the lithosphere over a region that is wider than the surface expression of RGR extension which is characterized by the well-defined normal faults and rift basins of the northern RGR (Murphy et al., 2024).

The gravity modelling results (***Figure 11***) show similar behavior in the lithosphere below Middle Park, Rabbit Ears Range, North Park and NW Colorado. The models show that the magmatic rocks present extend past the boundaries of the Middle and North Park Basins with synrift igneous rocks being located beneath the Park Range and Front Range. Additionally, towards the western end of the density model (***Figure 11***) the forward modelling showed that thinning in the upper crust was required to achieve a better gravity anomaly fit. The lateral extension of the synrift igneous rocks and the expression of crustal thinning obtained in the density model indicate that the lithosphere in the Park Basins region and NW Colorado might represent a transition from an early stage of rifting, with extension being accommodated over a wide area in northern Colorado, to a later, more advanced stage of rifting further south in the main RGR basins where extension is mainly accommodated along a narrow corridor bounded on one side by master normal faults. This is consistent with extension being more diffuse in northern Colorado where extensional faulting and volcanism is found to be more sparsely distributed over a wide area (Chapin & Cather, 1994; Kellogg, 1999).

6. SUMMARY

This thesis attempts to evaluate the possible presence of RGR related extension in northern Colorado, in the region located south of the Wyoming-Colorado state border where isolated basins such as Middle Park, North Park and Sand Wash Basins can be found. This region is immediately north of the Upper Arkansas River and Blue River Basins, the northernmost recognized RGR rift basins. Here, surface indicators of extension appear more widespread with faulting and late Tertiary volcanism that has developed synchronously with the main RGR basins. To evaluate possible RGR extension in northern Colorado, a forward gravity model was constructed to constrain the lithospheric and upper asthenosphere density structure.

The gravity data used was a combination of the PACES dataset (Keller et al., 2006) and 192 new gravity measurements collected west of the Park Basins region where the PACES data coverage is sparse. The Free Air Anomaly was calculated at 5000 m above all topographic features and the forward modelling software IGMAS+ (Schmidt et al., 2007) was employed to constrain the lithosphere density structure employing three E-W oriented cross sections that cut Middle Park, the Rabbit Ears Range and North Park, and extend longitudinally from the Front Range on the east towards the Utah-Colorado state border on the west. The general layered lithosphere structure used as a starting point for the forward model was derived from previous forward modelling work (Abdullin, 2012) and includes an upper and lower crust, a lithospheric mantle and the upper asthenosphere. Constraints obtained from previous work were used for the asthenosphere/lower crust boundary which was constrained from regional and local receiver function studies (Crosswhite & Humphreys, 2003b; Schmandt et al., 2015b). Sedimentary depths for the Middle and North Park Basins (Behrendt et al., 1969), Sand Wash Basin (Lickus & Law, 1988), Uinta Basin (Roberts, 2003) and Denver Basin (Hemborg, 1996) were constrained from existing structural maps. With these constraints applied, the forward gravity model shows a large amplitude, long wavelength gravity anomaly overestimation over the Park Basins region and a large amplitude, long wavelength gravity underestimation near the western end of the study area. This behavior is more pronounced towards the southern end of the

forward model in the Middle Park cross section reaching ~90 mGal overestimation and a ~80 mGal underestimation respectively.

The fit between the modeled and observed gravity profiles was improved in the Park Basins region by adding igneous intrusions at different depths within the lithosphere. The igneous features were added at the base of the lithosphere, lower crust and upper crust to accommodate the long and short wavelength component of the gravity anomaly respectively. These features include:

- A 2.8 g/cm^3 mafic igneous body that is present at the base of the lithosphere below the corridor defined by the Park Basins in all cross sections.
- Igneous bodies at the base of the Upper and Lower crust that become progressively more felsic northward from Middle Park (2.8 g/cm^3), through the Rabbit Ears (2.72 g/cm^3 and 2.8 g/cm^3), and into North Park (2.65 g/cm^3 and 2.79 g/cm^3).

The forward modelling process showed that these igneous features needed to have a smaller cross-sectional area towards the north end of the study area below North Park Basin in comparison to the south end below Middle Park Basin. The gravity anomaly long wavelength underestimation towards the western end of the study area was accommodated by including lateral density changes in the crust that are attributed to the transition from the Colorado Yavapai terrains to the denser Archean crust of Utah and the Wyoming craton.

These results provide valuable insight into the variation of the intrusive rock volume and composition from south to north in the study area and point to extension being accommodated in the lithosphere of the Park Basins area with more extension in the Middle Park area in comparison to the North Park area. The distribution of igneous rocks at the base of the lithosphere below the Park Basins area, correlates with previous geophysical observations that include shallowing of the Moho depth (Hansen et al., 2013) and lithosphere-asthenosphere boundary (LAB) (Levander et al., 2011) and low Vs and Vp seismic velocities (Levander et al., 2011; Schmandt et al., 2015b) in the Park Basins region. Together, these observations indicate that lithospheric thinning is present in the Park Basins region with more extension being accommodated in the Middle Park Basin lithosphere than in the North Park region and that

decompression melting has occurred in this region. The mafic igneous rocks in the Park Basins lithosphere can be interpreted as synrift magmatic intrusions produced by melting of fertile sources in the lithosphere mantle and/or upper asthenosphere without a considerable amount of extension. The prior history of subduction in the Colorado State area could have played an important role by placing these fertile sources beneath the Park Basins area during the tearing and foundering of the Farallon slab in the late stages of the Laramide orogenic period (Mayle & Harry, 2023; Ricketts et al., 2016). Finally, the discrepancy between the expression of extension throughout the depth of the lithosphere in the Park Basins region and the lack of localized extension in the surface similar to main RGR rift basins found in central Colorado and further south suggest a transition from an early stage of rifting in northern Colorado to greater amounts of extension (a more mature stage) further south.

6. BIBLIOGRAPHY

Abbey, A. L., & Niemi, N. A. (2018). Low-temperature thermochronometric constraints on fault initiation and growth in the northern Rio Grande rift, upper Arkansas River valley, Colorado, USA. *Geology*, *46*(7), 627–630. https://doi.org/10.1130/G40232.1

Abbey, A. L., & Niemi, N. A. (2020). Perspectives on Continental Rifting Processes From Spatiotemporal Patterns of Faulting and Magmatism in the Rio Grande Rift, USA. *Tectonics*, *39*(1), e2019TC005635. https://doi.org/10.1029/2019TC005635

Abdullin, A. (2012). *Geophysical Constraints on the Flexural Subsidence of the Denver Basin*. Colorado State University.

Behrendt, J. C., & Popenoe, P. (1969). Basement Structure Contour Map of North Park-Middle Park Basin, Colorado: GEOLOGICAL NOTES. *AAPG Bulletin*, *53*. https://doi.org/10.1306/5D25C6A7-16C1-11D7-8645000102C1865D

Behrendt, J. C., Popenoe, P., & Mattick, R. E. (1969). A Geophysical Study of North Park and the Surrounding Ranges, Colorado. *Geological Society of America Bulletin*, *80*(8), 1523. https://doi.org/10.1130/0016-7606(1969)80[1523:AGSONP]2.0.CO;2

Bjelotomić Oršulić, O., Varga, M., Markovinović, D., & Bašić, T. (2019). LTide - Matlab/Octave software tool for temporal and spatial analysis of tidal gravity acceleration effects according to Longman formulas. *Earth Science Informatics*, *12*(3), 405–414. https://doi.org/10.1007/s12145-019-00379-y

Brocher, T. M. (2005). Empirical Relations between Elastic Wavespeeds and Density in the Earth's Crust. *Bulletin of the Seismological Society of America*, *95*(6), 2081–2092. https://doi.org/10.1785/0120050077

Cather, S. M., Chapin, C. E., & Kelley, S. A. (2012). Diachronous episodes of Cenozoic erosion in southwestern North America and their relationship to surface uplift, paleoclimate, paleodrainage, and paleoaltimetry. *Geosphere*, *8*(6), 1177–1206. https://doi.org/10.1130/GES00801.1

Chapin, C. E., & Cather, S. M. (1994). Tectonic setting of the axial basins of the northern and central Rio Grande rift. In *Geological Society of America Special Papers* (Vol. 291, pp. 5–26). Geological Society of America. https://doi.org/10.1130/SPE291-p5

Cosca, M. A., Thompson, R. A., Lee, J. P., Turner, K. J., Neymark, L. A., & Premo, W. R. (2014). 40Ar/39Ar geochronology, isotope geochemistry (Sr, Nd, Pb), and petrology of alkaline lavas near Yampa, Colorado: Migration of alkaline volcanism and evolution of the northern Rio Grande rift. *Geosphere*, *10*(2), 374–400. https://doi.org/10.1130/GES00921.1

Crosswhite, J. A., & Humphreys, E. D. (2003a). Imaging the mountainless root of the 1.8 Ga Cheyenne belt suture and clues to its tectonic stability. *Geology*, *31*(8), 669. https://doi.org/10.1130/G19552.1

Crosswhite, J. A., & Humphreys, E. D. (2003b). Imaging the mountainless root of the 1.8 Ga Cheyenne belt suture and clues to its tectonic stability. *Geology*, *31*(8), 669. https://doi.org/10.1130/G19552.1

Eaton, G. P. (2013). A Plate-Tectonic Model for Late Cenozoic Crustal Spreading in the Western United States. In R. E. Riecker (Ed.), *Special Publications* (pp. 7–32). Washington, D. C.: American Geophysical Union. https://doi.org/10.1029/SP014p0007

Gibson, S. A., Thompson, R. N., Leat, P. T., Dickin, A. P., Morrison, M. A., Hendry, G. L., & Mitchell, J. G. (1992). Asthenosphere-derived magmatism in the Rio Grande rift, western USA: implications for continental break-up. *Geological Society, London, Special Publications*, *68*(1), 61–89. https://doi.org/10.1144/GSL.SP.1992.068.01.05

Glen, I. A. (1966). Tertiary Extrusive Volcanic Rocks in Middle Park, Grand County, Colorado. *Geological Surver Research*.

Götze, H. -J., & Lahmeyer, B. (1988). Application of three-dimensional interactive modeling in gravity and magnetics. *GEOPHYSICS*, *53*(8), 1096–1108. https://doi.org/10.1190/1.1442546

Hansen, S. M., Dueker, K. G., Stachnik, J. C., Aster, R. C., & Karlstrom, K. E. (2013). A rootless rockies—Support and lithospheric structure of the Colorado Rocky Mountains inferred from CREST and TA seismic data. *Geochemistry, Geophysics, Geosystems*, *14*(8), 2670–2695. https://doi.org/10.1002/ggge.20143

Hemborg, H. T. (1996). MS-30 Basement Structure Map of Colorado with Major Oil and Gas Fields. Colorado Geological Survey.

Hinze, W. J., Aiken, C., Brozena, J., Coakley, B., Dater, D., Flanagan, G., et al. (2005). New standards for reducing gravity data: The North American gravity database. *GEOPHYSICS*, *70*(4), J25–J32. https://doi.org/10.1190/1.1988183

Kaiser, W. R., Scott, A. R., Hamilton, D. S., Tyler, R., McMurry, R. G., Laubach, S. E., et al. (1992). *Geologic and Hydrologic Controls on Coalbed Methane: Sand Wash Basin, Colorado and Wyoming*. Bureau of Economic Geology.

Keller, G. R., & Baldridge, W. S. (1999). The Rio Grande rift: A geological and geophysical overview. *Rocky Mountain Geology*, *34*(1), 121–130. https://doi.org/10.2113/34.1.121

Keller, G. R., Hildenbrand, T. G., Kucks, R., Webring, M., Briesacher, A., Rujawitz, K., et al. (2006). A community effort to construct a gravity database for the United States and an associated Web portal. In A. K. Sinha, *Geoinformatics: Data to Knowledge*. Geological Society of America. https://doi.org/10.1130/2006.2397(02)

Kellogg, K. S. (1999). Neogene basins of the northern Rio Grande rift: partitioning and asymmetry inherited from Laramide and older uplifts. *Tectonophysics*, *305*(1–3), 141–152. https://doi.org/10.1016/S0040-1951(99)00013-X

Kreemer, C., Blewitt, G., & Bennett, R. A. (2010). Present-day motion and deformation of the Colorado Plateau. *Geophysical Research Letters*, *37*(10), 2010GL043374. https://doi.org/10.1029/2010GL043374

Landman, R. L., & Flowers, R. M. (2013). (U-Th)/He thermochronologic constraints on the evolution of the northern Rio Grande Rift, Gore Range, Colorado, and implications for rift propagation models.

Levander, A., Schmandt, B., Miller, M. S., Liu, K., Karlstrom, K. E., Crow, R. S., et al. (2011). Continuing Colorado plateau uplift by delamination-style convective lithospheric downwelling. *Nature*, *472*(7344), 461–465. https://doi.org/10.1038/nature10001

Lickus, M. R., & Law, B. E. (1988). *Structure contour map of the greater Green River basin, Wyoming, Colorado, and Utah*. https://doi.org/10.3133/mf2031

Livaccari, R. F. (1979). Late Cenozoic tectonic evolution of the western United States. *Geology*, *7*(2), 72. https://doi.org/10.1130/0091-7613(1979)7<72:LCTEOT>2.0.CO;2

Mayle, M., & Harry, D. L. (2023). Syn-Rift Magmatism and Sequential Melting of Fertile Lithologies in the Lithosphere and Asthenosphere. *Journal of Geophysical Research: Solid Earth*, *128*(9), e2023JB027072. https://doi.org/10.1029/2023JB027072

Morgan, P., Seager, W. R., & Golombek, M. P. (1986). Cenozoic thermal, mechanical and tectonic evolution of the Rio Grande Rift. *Journal of Geophysical Research: Solid Earth*, *91*(B6), 6263–6276. https://doi.org/10.1029/JB091iB06p06263

Moucha, R., Forte, A. M., Rowley, D. B., Mitrovica, J. X., Simmons, N. A., & Grand, S. P. (2008). Mantle convection and the recent evolution of the Colorado Plateau and the Rio Grande Rift valley. *Geology*, *36*(6), 439. https://doi.org/10.1130/G24577A.1

Murphy, B. S., Caine, J. S., Bedrosian, P. A., & Crosbie, J. W. (2024). Geoelectric evidence for a wide spatial footprint of active extension in central Colorado. *Geology*. https://doi.org/10.1130/G51517.1

Murray, K. D., Murray, M. H., & Sheehan, A. F. (2019). Active Deformation Near the Rio Grande Rift and Colorado Plateau as Inferred from Continuous Global Positioning System Measurements. *Journal of Geophysical Research: Solid Earth*, *124*(2), 2166–2183. https://doi.org/10.1029/2018JB016626

Raynolds, R. G., & Hagadorn, J. W. (2017). *MS-53 Colorado Stratigraphy Chart*. Colorado Geological Survey. https://doi.org/10.58783/cgs.ms53.cxwh3412

Ricketts, J. W., Kelley, S. A., Karlstrom, K. E., Schmandt, B., Donahue, M. S., & Van Wijk, J. (2016). Synchronous opening of the Rio Grande rift along its entire length at 25–10 Ma supported by apatite (U-Th)/He and fission-track thermochronology, and evaluation of possible driving mechanisms. *Geological Society of America Bulletin*, *128*(3–4), 397–424. https://doi.org/10.1130/B31223.1

Roberts, L. N. R. (2003). Structure Contour Map of the Top of the Dakota Sandstone, Uinta-Piceance Province, Utah and Colorado. US Geological Survey. Retrieved from https://pubs.usgs.gov/dds/dds-069/dds-069-b/REPORTS/Chapter_16.pdf

Rumpfhuber, E., & Keller, G. R. (2009). An integrated analysis of controlled and passive source seismic data across an Archean-Proterozoic suture zone in the Rocky Mountains. *Journal of Geophysical Research: Solid Earth*, *114*(B8), 2008JB005886. https://doi.org/10.1029/2008JB005886

Russell, L. R., & Snelson, S. (1994). Structure and tectonics of the Albuquerque Basin segment of the Rio Grande rift: Insights from reflection seismic data. In *Geological Society of America Special Papers* (Vol. 291, pp. 83–112). Geological Society of America. https://doi.org/10.1130/SPE291-p83

Schmandt, B., Lin, F., & Karlstrom, K. E. (2015a). Distinct crustal isostasy trends east and west of the Rocky Mountain Front. *Geophysical Research Letters*, *42*(23). https://doi.org/10.1002/2015GL066593

Schmandt, B., Lin, F., & Karlstrom, K. E. (2015b). Distinct crustal isostasy trends east and west of the Rocky Mountain Front. *Geophysical Research Letters*, *42*(23). https://doi.org/10.1002/2015GL066593

Schmidt, S., Götze, H.-J., Fichler, Ch., Ebbing, J., & R. Alvers, M. (2007). 3D Gravity, FTG and Magnetic Modeling: the new IGMAS+ Software. In *EGM 2007 International Workshop*. Capri, Italy,: European Association of Geoscientists & Engineers. https://doi.org/10.3997/2214-4609-pdb.166.D_PP_06

Seager, W. R., & Morgan, P. (1979). Rio Grande Rift in Southern New Mexico, West Texas, and Northern Chihuahua. In R. E. Riecker (Ed.), *Special Publications* (pp. 87–106). Washington, D. C.: American Geophysical Union. https://doi.org/10.1029/SP014p0087

Sosa, A., Thompson, L., Velasco, A. A., Romero, R., & Herrmann, R. B. (2014). 3-D structure of the Rio Grande Rift from 1-D constrained joint inversion of receiver functions and surface wave dispersion. *Earth and Planetary Science Letters*, *402*, 127–137. https://doi.org/10.1016/j.epsl.2014.06.002

Tweto, O. (1976). Geologic Map of the Craig 1 x 2 Quadrangle, Northwestern Colorado. United States Geological Survey.

U.S. Geological Survey. (2024). 3D Elevation Program (3DEP) 1/3 arc-second DEM [Data set]. Retrieved from https://apps.nationalmap.gov/downloader/

Van Wijk, J., Van Hunen, J., & Goes, S. (2008). Small-scale convection during continental rifting: Evidence from the Rio Grande rift. *Geology*, *36*(7), 575. https://doi.org/10.1130/G24691A.1

Weil, A. B., & Yonkee, A. (2023). The Laramide orogeny: Current understanding of the structural style, timing, and spatial distribution of the classic foreland thick-skinned tectonic system. In S. J. Whitmeyer, M. L. Williams, D. A. Kellett, & B. Tikoff, *Laurentia: Turning Points in the Evolution of a Continent* (pp. 707–771). Geological Society of America. https://doi.org/10.1130/2022.1220(33)

Whitmeyer, S. J., & Karlstrom, K. E. (2007). Tectonic model for the Proterozoic growth of North America. *Geosphere*. https://doi.org/10.1130/GES00055.1

Wilson, D., Aster, R., Ni, J., Grand, S., West, M., Gao, W., et al. (2005). Imaging the seismic structure of the crust and upper mantle beneath the Great Plains, Rio Grande Rift, and Colorado Plateau using receiver functions. *Journal of Geophysical Research: Solid Earth*, *110*(B5), 2004JB003492. https://doi.org/10.1029/2004JB003492